ISRMC-MAC: Implementable Single-Radio, Multi-Channel MAC Protocol for WBANs

Kunryun Cho[1], Seokhee Jeon[2], Jinsung Cho[3] and Ben Lee[4]
[1-3]Dept. Of Computer Engineering, Kyung Hee University
Yongin, Gyeonggi-do - Korea
[e-mail: whrjsfbs@gmail.com][1]
[e-mail: jeon@khu.ac.kr][2]
[e-mail: chojs@khu.ac.kr][3]
[2] School of Electrical Engineering and Computer Science, Oregon State University
Corvallis, OR 97330 - USA
[e-mail: benl@eecs.orst.edu]
*Corresponding author: Jinsung Cho

Received March 3, 2015; revised June 5, 2015; accepted October 15, 2015; published March 31, 2016

Abstract

Wireless Body Area Networks (WBANs) have received a lot of attention as a promising technology for medical and healthcare applications. A WBAN should guarantee energy efficiency, data reliability, and low data latency because it uses tiny sensors that have limited energy and deals with medical data that needs to be timely and correctly transferred. To satisfy this requirement, many multi-radio multi-channel MAC protocols have been proposed, but these cannot be implemented on current off-the-shelf sensor nodes because they do not support multi-radio transceivers. Thus, recently single-radio multi-channel MAC protocols have been proposed; however, these methods are energy inefficient due to data duplication. This paper proposes a TDMA-based single-radio, multi-channel MAC protocol that uses the Unbalanced Star+Mesh topology to satisfy the requirements of WBANs. Our analytical analysis together experiments using real sensor nodes show that the proposed protocol outperforms existing methods in terms of energy efficiency, reliability, and low data latency.

Keywords: WBAN, multi-channel MAC, Unbalanced Star+Mesh topology, GTS allocation

A preliminary version of this paper appeared in ACM ICUIMC 2014, Siem Reap, Cambodia (best paper award). This version includes the modification of the algorithm and its concrete analysis with implementation results on ZigbeX sensor nodes. This work was supported by the Basic Science Research Program through the National Research Foundation of Korea within the Ministry of Education under Grant NRF-2013R1A1A2059741.

http://dx.doi.org/10.3837/tiis.2016.03.006 **ISSN : 1976-7277**

1. Introduction

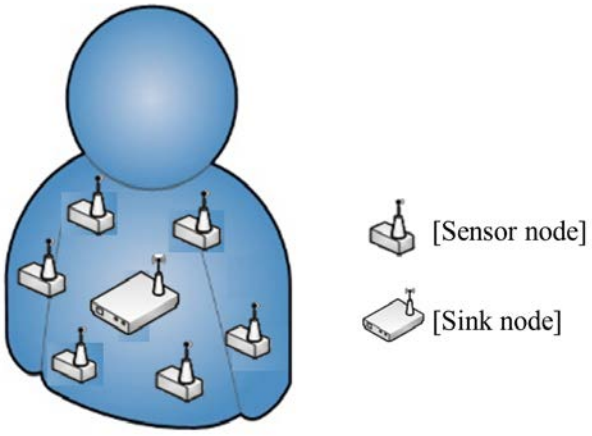

Fig. 1. Wireless Body Area Network.

Life expectancy has increased due to advances in medical technology. As such, many countries are faced with an aging society, and thus, using *Wireless Body Area Networks* (WBANs) in health care has gained a great deal of attention [1]. **Fig. 1** shows an example of a WBAN, which consists of a *sink node* and *sensor nodes*. A WBAN provides continuous monitoring of body condition and real-time feedback for medical diagnosis and consultations. This is realized using tiny sensors positioned in, on, or around a human body to measure biological data and communicate with other sensor nodes operating on ISM (2.4 GHz) and MICS (402-405 MHz) bands.

There are three important requirements for WBANs, which are *energy efficiency*, *reliability*, and *low latency*. These requirements also apply to Wireless Sensor Networks (WSNs), and thus, many protocols developed for WSNs have been applied to WBANs. For example, WBANs initially relied on contention-based single-channel MAC protocols that were originally proposed for WSNs [2-9]. However, these techniques do not fully satisfy the requirements of WBANs because WSNs consider communications over a large space, whereas WBANs consider communications over a small space with densely deployed sensor nodes. This leads to frequent collisions resulting in high latency and energy consumption. To reduce collisions, TDMA-based single-channel MAC protocols were proposed [10-12], but they cannot guarantee low latency because nodes have to wait for their allocated time slots to communicate. The multi-channel approach mitigates this inefficiency by enabling sensor nodes to communicate with each other through multiple channels. Several *multi-channel MAC protocols* for WBANs have been proposed that employ either *single radio* or *multi-radio*. **Fig. 2a** shows a multi-radio approach that utilizes multiple channels and antennas to communicate concurrently and thus increase channel efficiency. However, this approach cannot be realized using off-the-shelf sensor devices since they do not support multiple radios. On the other hand, single-radio with multiple channels shown in **Fig. 2b** is already supported by off-the-shelf sensor devices. However, special topology and collision prevention mechanism are needed to trade-off between latency and energy efficiency.

In order to understand this trade-off, **Fig. 3** compares the existing single-radio MAC protocols that can be categorized into *TDMA-based single-channel star topology* and

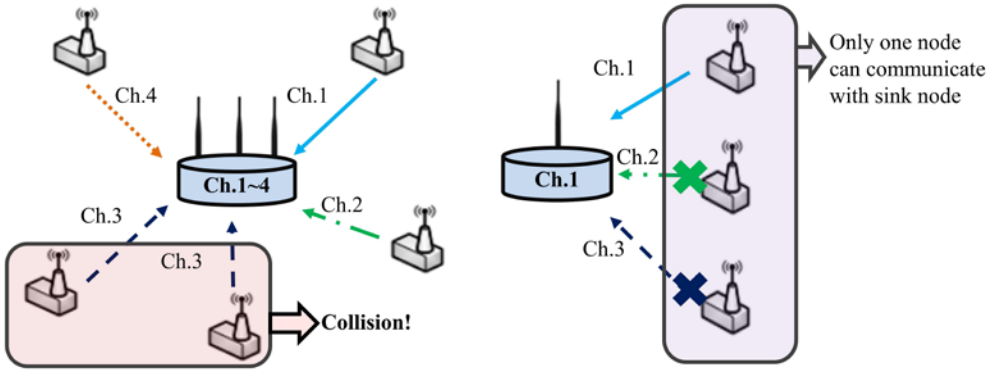

(a) Multi-radio, multi-channel. (b) Single-radio, multi-channel.

Fig. 2. Two types of multi-channel MAC protocols.

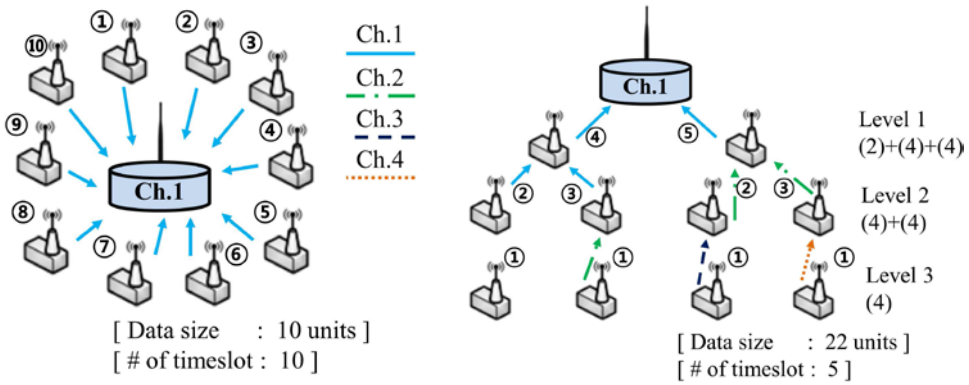

(a) Single-channel. (b) Multi-channel.

Fig. 3. Existing single-radio MAC protocols and topologies.

TDMA-based multi-channel tree topology. In these figures, all of the sensor nodes are assumed to transmit one unit data to the sink node. When a node transmits data to the sink node during its allocated time slot, the other nodes go into a sleep state, and all the nodes perform this process sequentially. However, latency increases since the nodes have to wait for their allocated time slots. On the other hand, the TDMA-based multi-channel tree topology shown in **Fig. 3b** can decrease latency. This is because when a node communicates with the sink node during its allocated time slot, other nodes aggregate data to their parent nodes. This reduces the number of time slots used, but data duplication occurs leading to energy inefficiency.

This paper proposes the *Implementable Single-Radio Multi-Channel MAC* (ISRMC-MAC) protocol that uses a TDMA-based single-radio, multi-channel approach to resolve the aforementioned problems. As mentioned before, previous single-radio, multi- channel MAC protocols trade off between energy efficiency and latency. In contrast, the proposed ISRMC-MAC protocol provides not only low latency but also high energy efficiency. This is achieved by employing a new topology called *Unbalanced Star+Mesh topology*, which reduces the total number of utilized time slots leading to lower latency. Moreover, it results in minimum hop transmission reducing data duplication. Thus, energy efficiency increases

compared with existing single-radio, multi-channel MAC protocols. The proposed ISRMC-MAC protocol has been implemented on off-the-shelf sensor nodes, called ZigbeX.

The rest of this paper is organized as follows. Section 2 briefly discusses the related work on multi-channel MAC protocols and Section 3 proposes the ISRMC-MAC protocol. Performance evaluation is presented in Section 4 and Section 5 concludes the paper.

2. Related Work

Mutli-channel MAC protocols have received a lot of attention as a promising solution to increase throughput. However, most of the existing multi-channel based protocols have been proposed for WSNs [13], and a few of them are suitable for WBANs [14,15]. These protocols can be categorized into single-radio and multi-radio as shown in **Fig. 2**. Both methods provide multiple channels, but single-radio cannot provide concurrent communications because the sink node has only one transceiver. To overcome this limitation, single-radio, multi-channel MAC protocols require special topology and algorithm. The following subsections present several existing single-radio and multi-radio multi-channel MAC protocols.

2.1 Single-Radio, Multi-Channel MAC Protocols

Kim *et al.* proposed Y-MAC [16] that uses a frequency hopping mechanism based on broadcast and unicast periods. Each node transmits and receives data at its own time slot. However, if a node cannot transmit all of its data in a single time slot, frequency hopping is performed to transmit the remaining data. Incel *et al.* proposed the Multi-Channel Lightweight MAC Protocol (MC-LMAC) [17], which is based on the single-channel LMAC [18]. If the distance between sensor nodes is shorter than three hops, they are assigned to different time slots and channels. However, Y-MAC and MC-LMAC are not suitable for WBANs because they depend on a distributed architecture. Multi-frequency MAC protocol for wireless Sensor Network (MMSN) [19] improves the channel efficiency using frequency assignment and media access mechanism based on a tree topology. Hybrid MAC (HyMAC) [20] and Low-overhead Multi-channel MAC protocol (MuChMAC) [21] also employ the tree topology to solve the bottleneck problem at the sink node. If nodes have the same parent, they are assigned different time slot, and if nodes are assigned the same time slot, they are allocated to different frequencies. MMSN, HyMAC, and MuChMAC can all guarantee high throughput but the aggregation and redundant transmission of data will lead to energy inefficiency as shown in **Fig. 3b**.

2.2 Multi-Radio, Multi-Channel MAC Protocols

Single-radio, multi-channel MAC protocols improve channel efficiency, but they suffer from energy inefficiency because the tree topology they require leads to data duplication. To solve this problem, some protocols rely on multiple transceivers. Tree-based Multi-Channel Protocol (TMCP) [22] constructs a tree topology with the sink node representing the root. The sink node has multiple transceivers and each child node of the sink node can transmit data using a different channel. Cluster On-demand Multi-channel MAC (COMMAC) [23] is a cluster-based protocol that is organized as a three-tier architecture consisting of the sink node, aggregators, and sensor nodes. The aggregators receive data from the sensor nodes using multiple transceivers and transmit them to the sink node. Lee *et al.* proposed a MAC protocol [24] that uses two kinds of nodes, outbody and inbody nodes. An outbody node assigns channels to inbody nodes and receives data from inbody nodes using multiple transceivers. Kirbas *et al.* proposed isMAC [25] that uses a single-radio by default, but the coordinator node

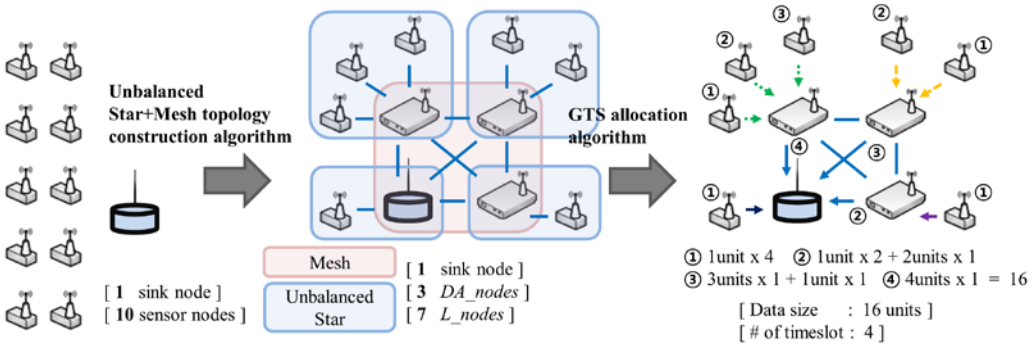

Fig. 4. Overview of the ISRMC-MAC protocol.

can change to the multi-radio mode to improve channel efficiency when an emergency situation occurs. However, isMAC requires multiple transceivers, and thus, it cannot be realized using off-the-shelf sensor devices.

In summary, existing multi-channel MAC protocols have the following shortcomings: For single-radio approach, a trade-off exists between energy consumption and throughput. On the other hand, multi-radio approach is impracticable using commercial off-the-shelf sensor devices. In order to overcome these problems, the proposed ISRMC-MAC protocol takes the single-radio approach and employs the *unbalanced Star+Mesh topology* and TDMA-based transmission mechanism.

3. The proposed ISRMC-MAC Protocol

There are three kinds of nodes in ISRMC-MAC: the sink node, Data Aggregation nodes (*DA_nodes*), and Leaf nodes (*L_nodes*). The sink node and *DA_nodes* form a mesh topology and have *L_nodes* as their leaves in a star topology. This hybrid topology is referred to as '*unbalanced Star+Mesh*' because the number of leaf nodes that *DA_nodes* may have can be different. The topology construction algorithm is described in Subsection 3.1. As for the transmission mechanism, *L_nodes* first transmit data to their parents, i.e., *DA_nodes*. Then, *DA_nodes* aggregate the received data with their own data and transmit them to the sink node through the mesh network. **Fig. 4** illustrates the overall process of ISRMC-MAC assuming that each sensor node transmits one unit of data, and the number of channels and the number of sensor nodes are 4 and 10, respectively. In addition, the circled numbers indicate the starting time slots for the messages and different arrows represent different channels. Note that the number of channels and the number of nodes in **Fig. 4** are equivalent to those in **Fig. 3b.** Therefore, the total amount of data and the number of time slots required for transmission in **Fig. 4** are reduced compared with **Fig. 3b.** This indicates that ISRMC-MAC improves communication throughput and energy efficiency.

The following subsections discuss the construction of the *Unbalanced Star+Mesh topology* and the Guaranteed Time Slots (GTS) allocation algorithm.

3.1 Unbalanced Star+Mesh topology construction

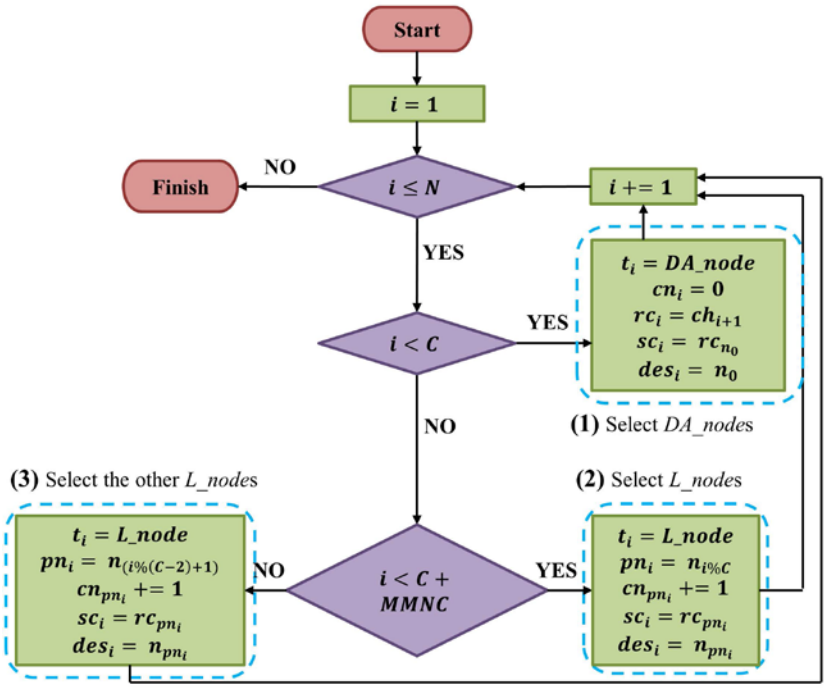

Fig. 5. Flowchart for unbalanced Star+Mesh topology construction.

Table 1 defines the notations used throughout this subsection. **Fig. 5** shows the flowchart for the construction of the *Unbalanced Star+Mesh topology*. Moreover, it is assumed that all the nodes can communicate with each other using their lowest transmission power since they are placed in/on/around human body.

The network consists of the sink node n_0, N sensor nodes (n_1, n_2, ⋯, n_N), and C channels (ch_1, ch_2, ⋯, ch_C). Furthermore, the sink node's receiving channel (rc_0) is ch_1. The first step involves the selection of *DA_nodes*. For each n_i, where i is less than C, its node type (t_i) becomes *DA_node* and the number of child nodes it has (cn_i) is initialized to 0. In addition, its receiving channel (rc_i) and sending channel (sc_i) are set to ch_{i+1} and ch_1, respectively. Finally, its destination node (des_i) becomes n_0 since the destination node for *DA_nodes* is the

Table 1. Notation used in **Fig. 5**.

Notation	Definition
C	Number of channels
N	Number of nodes
n_0	Sink node
n_i	Sensor node i (n_1~n_N)
ch_j	Channel j (ch_1~ch_C)
t_i	Node type of n_i
pn_i	Parent node of n_i
cn_i	Number of child nodes for n_i
sc_i	Sending channel of n_i
rc_i	Receiving channel of n_i
des_i	Destination of n_i

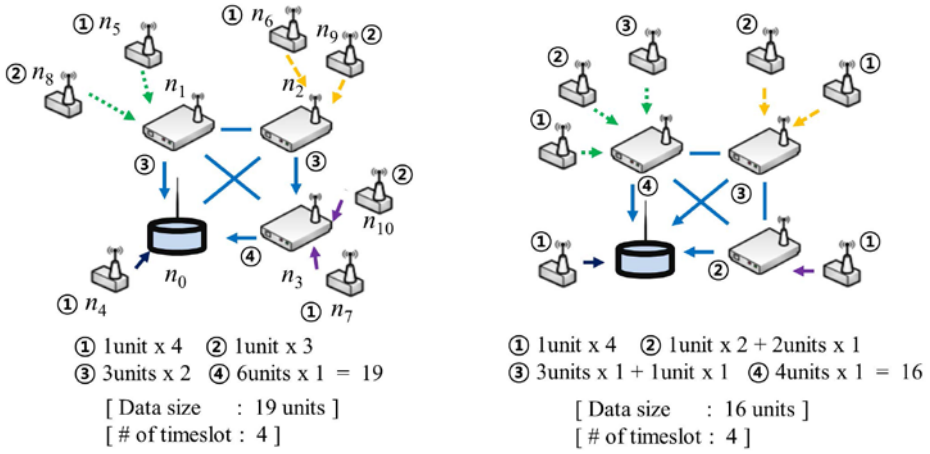

(a) When the last DA_node takes the remaining node. (b) The proposed topology.

Fig. 6. The reason why the last *DA_node* is excluded from the selection of the remaining *L_nodes.*

sink node.

The second step involves the selection of *L_nodes*. This is done for each node n_i, where i greater than or equal to C and less than $C + MMNC$. $MMNC$ represents the *maximum multiple number of channels*, which is less than $N - (C - 1)$, and expressed as $\lfloor (N - (C - 1))/C \rfloor \times$ C. For each of these nodes, its node type (t_i) is set to *L_node* and its parent node (pn_i) is set to $n_{i\%C}$. These *L_nodes* then join the mesh network that consists of the sink node and leaf nodes $n_1 \sim n_{C-1}$. As each *L_node* joins the mesh network, the number of child nodes its parent node has (cn_{pn_i}) is increased by one. In addition, its sending channel (sc_i) and destination node (des_i) are set to the receiving channel of its parent node (rc_{pn_i}) and its parent node (n_{pn_i}), respectively. Note that if there are more than one *DA_nodes* ready to transmit data to the sink node at the same time, data transmission needs to be performed sequentially causing latency to increase. In this case, *DA_nodes* collect data from each other via the mesh topology. Thus, their sending channel (sc_i) and destination (des_i) need to be changed, which will be explained in detail in Section 3.2.

The final step is the selection of the rest of *L_nodes*. This is done for each node n_i, where i is larger than or equal to $C + MMNC$ and less then or equal to N. For each these nodes, its node type (t_i) is set to *L_node* and its parent node (pn_i) is set to $n_{(i\%(C-2))+1}$. The remaining nodes join the *DA_nodes* except the last *DA_node* (i.e., n_{C-1}). This is done to reduce data aggregation and to exploit parallelism, and will be explained shortly. The rest of the information cn_{pn_i}, sc_i, and des_i are determined the same way as the second step.

Fig. 6 illustrates the reason why the last *DA_node* is excluded from the selection of the remaining *L_nodes*. If the remaining *L_nodes* are assigned to the last *DA_node* as shown in **Fig. 6a**, the sink node will be idle while nodes n_1, n_2, and n_3 receive data from nodes n_8, n_9, and n_{10}, respectively. More specifically, during the first time slot, n_4, n_5, n_6, and n_7 transmit their data during the first time slot in each channel to n_0 n_1, n_2, and n_3, respectively. During the second time slot, n_8, n_9, n_{10} transmit to n_1, n_2, n_3, respectively. During the third time slot, n_1 delivers the aggregated data from n_1, n_5, and n_8 to the sink node, and n_2 delivers the aggregated data from n_2, n_6, and n_9 to n_3. During the final time slot, n_3 delivers the aggregated data from n_2, n_3, n_6, n_7, n_9, and n_{10} to the sink node. Therefore, a total 19 units

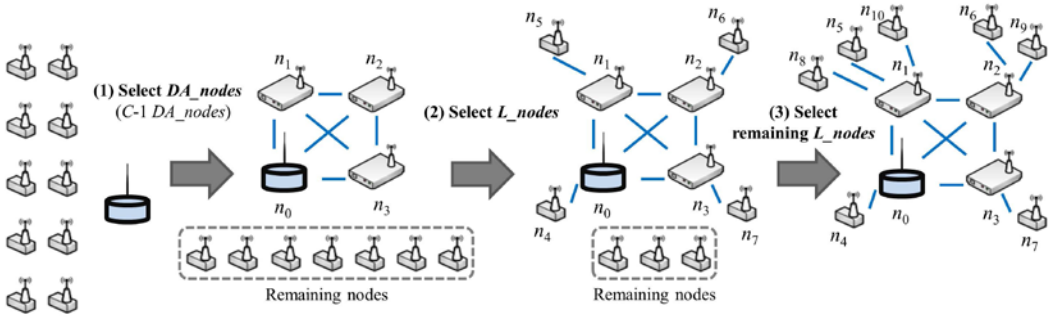

Fig. 7. An example construction of an Unbalanced Star+Mesh topology

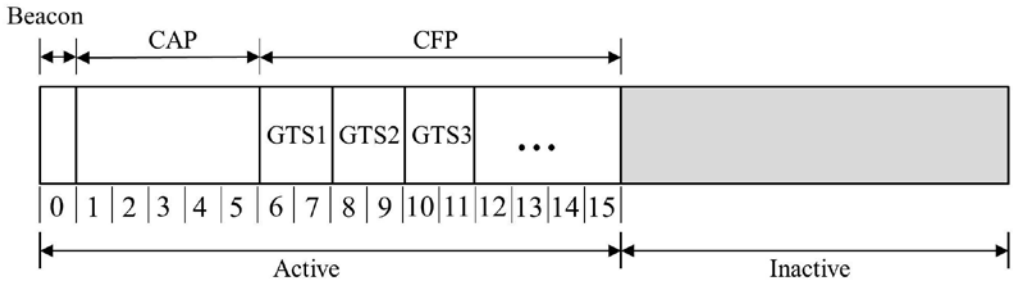

Fig. 8. Superframe structure in IEEE 802.15.4.

of data are transmitted. However, in our proposed topology shown in **Fig. 6b**, n_3 can deliver the aggregated data to n_7 during the second time slot, while n_1 and n_2 aggregate data from their *L_nodes*. Thus, the total data size can be reduced to 16 units in the proposed method.

Fig. 7 shows the construction of an example *Unbalanced Star+Mesh topology* for $C = 4$ and $N = 10$. In the first step, sensor nodes n_1 through n_3 are selected as *DA_nodes*. This is done by setting the receiving channels for nodes n_1, n_2, and n_3 to ch_2, ch_3, and ch_4, respectively. Moreover, the sending channels for the *DA_nodes* are set to ch_1, and the destination is set to n_0. In the second step, the sink node and *DA_nodes* are each assigned the same number of *L_nodes*. Thus, the sensor nodes n_4 is assigned to the sink node n_0, and sensor nodes n_5, n_6, and n_7 are assigned to *DA_nodes* n_1, n_2, and n_3, respectively. In addition, the sending channels for nodes n_4, n_5, n_6, and n_7 are set to ch_1, ch_2, ch_3, and ch_4, respectively. In the last step, the remaining sensor nodes n_{C+MMNC} through n_N are sequentially assigned to *DA_nodes* except the last *DA_node* (i.e., n_{C-1}), which is done to reduce data aggregation and exploit parallelism.

The proposed method also conisders the residual energy of nodes. As can be seen in **Fig.6**, *DA_nodes* consume more energy than *L_nodes* since they aggregate data from *L_nodes* and transmit it to the sink node. In constrast, *L_nodes* only transmit data to a *DA_node*. This imbalance in energy consumption requires the role between *DA_node* and *L_node* to be swapped, and thus, the topology construction in **Fig. 5** is performed periodically. The sink node collects the residual energy of all the nodes and the node number in **Fig. 5** is given in descending order of its residual energy.

3.2 GTS Allocation Algorithm

The proposed GTS allocation algorithm can be applied to any time slot TDMA-based protocols; however, our discussion is based on IEEE 802.15.4 packet frame and superframe

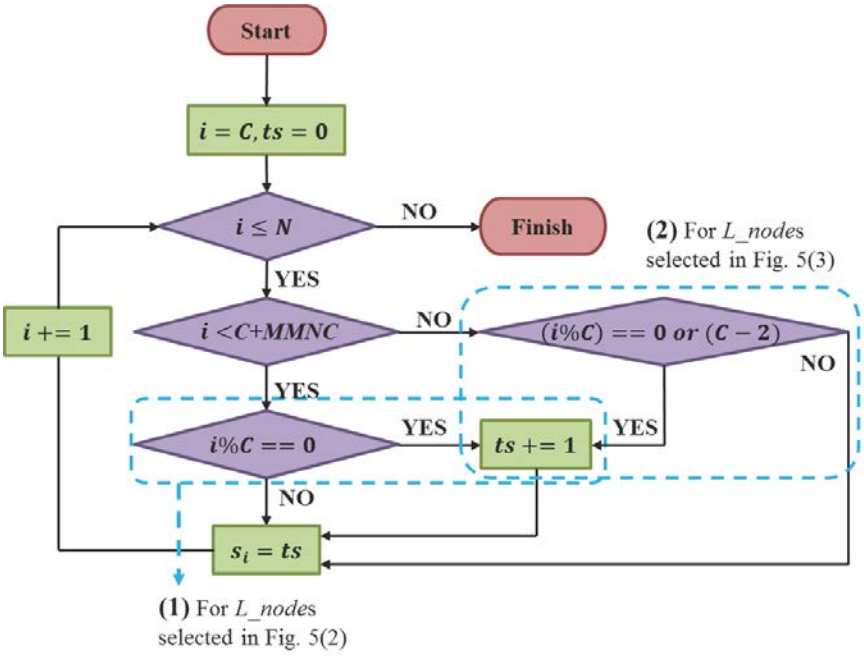

Fig. 9. GTS allocation for *L_nodes*.

structure [26]. The superframe structure is shown in **Fig. 8**, which is composed of Active and Inactive periods. The Active period is subdivided into beacon period, Contention Access Period (CAP), and Contention Free Period (CFP). During the beacon period, the sink node broadcasts a beacon signal to synchronize all the sensor nodes. After the beacon period, all the nodes except the sink node communicate data during the CAP based on the slotted CSMA/CA. During the CFP, nodes use their Guaranteed Time Slots (GTSs) to transmit data without collisions. The Inactive period is the same as the sleep period. The CFP can reduce unnecessary collisions and retransmissions, which are the causes of energy inefficiency. Thus, the proposed ISRMC-MAC protocol employs only the beacon period and the CFP in the superframe structure.

The overall process of the GTS allocation is as follows: The first part of the GTSs in each channel is allocated to *L_nodes* for transmiting data to their parent nodes (i.e., *DA_nodes*). The next part of the GTSs is used for *DA_nodes* to deliver the aggregated data either to the sink node in the tree topology or to the other *DA_nodes* in the mesh topology. **Table 2** shows the notations used in the GTS allocation algorithm.

Fig. 9 shows the flowchart of the GTS allocation algorithm for *L_nodes*. First, the time slots from the beginning of the CFP are allocated to *L_nodes* that were selected during the second step of the *Unbalanced Star+Mesh topology* construction shown in **Fig. 5**. This is

Table 2. Notation used in **Fig. 9** and **Fig. 10**.

Notation	Definition
t_s	GTS time slot
s_i	GTS time slot number of n_i
DA_S	A set of *DA_nodes* for GTS allocation
n_{HCN}	Node in DA_S with maximum number of child nodes
n_{LCN}	Node in DA_S with minimum number of child nodes

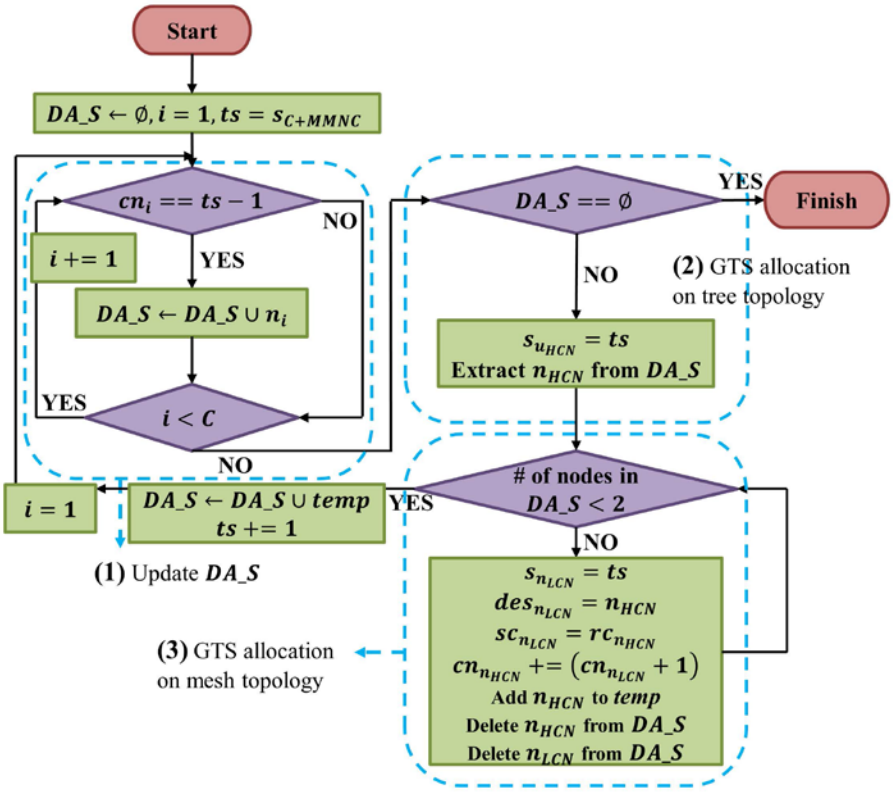

Fig. 10. GTS allocation for *DA_nodes*.

done for each n_i, where i is greater than equal to C and less than $C + MMNC$. For each node that satisfies this requirement, the 1^{st} time slot (ts) is assigned as the time slot number for n_i (s_i). Although ts starts with 0, it is incremented by one (i.e., the first time slot) in the first iteration because i starts with C (i.e., $i\%C == 0$). After these *L_nodes* have been assigned to the 1^{st} time slot, ts is incremented by one. This process repeats until there are less than C nodes remaining. Next, the remaining *L_nodes* that were selected during the last step in **Fig. 5** are allocated to the time slot. Since the remaining *L_nodes* are assigned to *DA_nodes* except the last *DA_node* (i.e., nodes n_1, n_2, $\cdots$, n_{C-2}), both n_{C+MMNC} and $n_{C+MMNC+C-2}$ are assigned to n_1. Therefore, ts is increased by one when $i\%C$ is equal to either 0 or $C - 2$.

The flowchart for the GTS allocation for *DA_nodes* is given in **Fig. 10**. The algorithm starts with ts initialized to s_{C+MMNC} and an empty set of *DA_nodes* (*DA_S*). In the first step, a check is made to determine whether each *DA_node* has aggregated all the data from its *L_nodes*. This is done by checking whether the number of child nodes it has (cn_i) is equal to the previous time slot $ts - 1$. If so, the *DA_node* has aggregate data from all of its *L_nodes*, and the node n_i is added to the set of *DA_nodes* (*DA_S*). This process is repeated as long as i is less than C.

In the second step, if *DA_S* is not empty, it means one or more *DA_nodes* are ready to send data to the sink node at time slot ts, thus conflicts may occur because the sink node uses just a single channel. Therefore, the *DA_node* that has the largest number of child nodes among

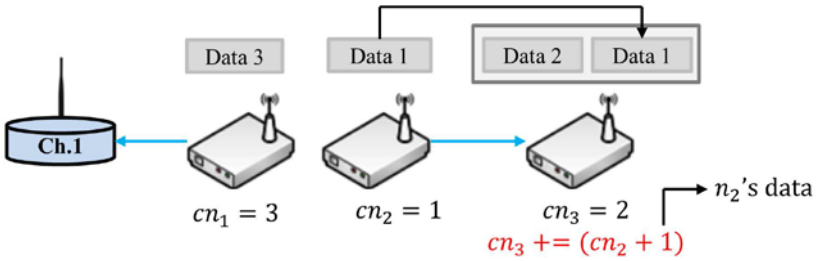

Fig. 11. Data transmission of *DA_nodes* in Unbalanced Star+Mesh topology.

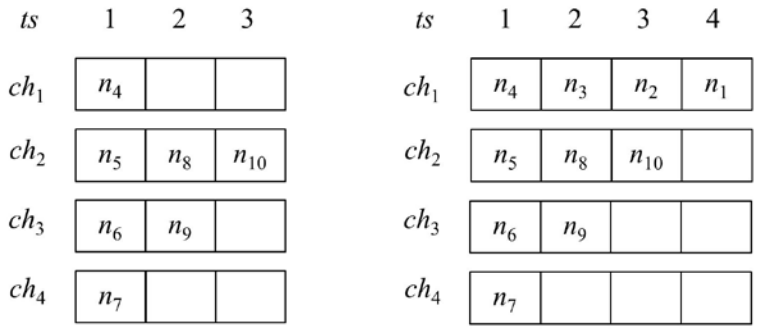

(a) After *L_nodes*. (b) After *DA_nodes*.

Fig. 12. An Example of GTS allocation.

DA_nodes in *DA_S* (n_{HCN})[1] is allocated the current time slot (ts), and then it is removed from *DA_S*.

The third step involves the GTS allocation on the mesh topology. If there are two or more nodes in *DA_S*, communication parallelism among the *DA_nodes* can be utilized on the mesh topology. In other words, *DA_nodes* in *DA_S* may aggregate data among them. To do this, n_{HCN} and n_{LCN} are first selected, and then n_{LCN} delivers its data to n_{HCN}. Therefore, the destination node des_{LCN} and the sending channel sc_{LCN}, which were determined by the topology construction algorithm, need to be changed to n_{HCN} and rc_{HCN}, respectively. This is achieved by the following set of operations: The time slot number for the node with the minimum number of child nodes ($s_{n_{LCN}}$) is set to the current time slot (ts), the destination for n_{LCN} ($des_{n_{LCN}}$) is set as n_{HCN}, the sending channel of n_{LCN} ($sc_{n_{LCN}}$) is set to the receiving channel of n_{HCN} ($rc_{n_{HCN}}$), and the maximum number of child nodes for n_{HCN} ($cn_{n_{HCN}}$) is increased by the number of child nodes for n_{LCN} ($cn_{n_{LCN}}$) plus one. Finally, n_{HCN} is moved to *temp* and both n_{HCN} and n_{LCN} are removed from *DA_S*. This process is repeated until the number of elements in *DA_S* is less than 2. When this occurs, the node in *temp* is added to *DA_S* and the time slot is incremented by one. Then, the entire process is repeated until *DA_S* becomes empty.

Fig. 11 illustrates an example of data transmission of *DA_nodes* in the *Unbalanced Star+Mesh topology*. In this figure, $DA\_S = \{n_1, n_2, n_3\}$ after the first step, n_1 is selected as n_{HCN} in the second step, and its destination is the sink node. In the third step, n_3 and n_2 are

[1] When there are ties, the DA_node that has the smallest number wins.

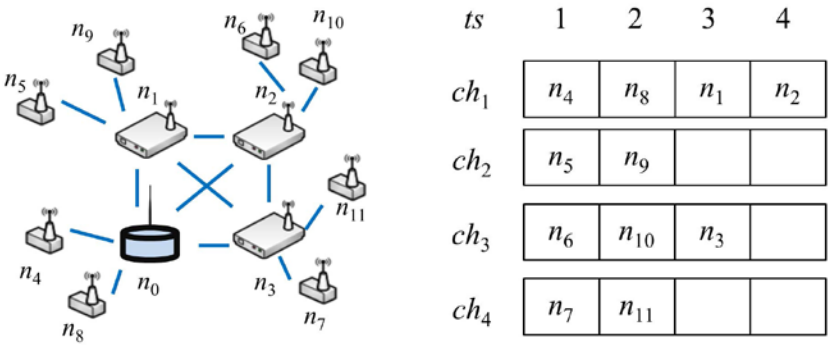

(a) Topology. (b) GTS allocation.

Fig. 13. Another Example of GTS allocation.

selected as n_{HCN} and n_{LCN}, respectively, and then n_2 transmits its data to n_3 while n_1 delivers its data to the sink node.

Fig. 12 depicts an example of GTS allocation process for the *Unbalanced Star+Mesh topology* constructed in **Fig. 7**. **Fig. 12a** shows the GTS allocation for the *L_nodes*. This information can also be used to determine when a *DA_node* has aggregated data from its *L_nodes*. For example, when $ts = 2$, only n_3 has aggregated all the data from its *L_nodes* since cn_3 is 1, and thus, *DA_S* = $\{n_3\}$ after the first step. **Fig. 12b** shows the GTS allocation for the *DA_nodes*. For example, when $ts = 2$, the time slot is allocated to n_3 based on step (2) of **Fig. 10** because *DA_S* = $\{n_3\}$. After the second step, *DA_S* is empty and thus the first step of the algorithm repeats with $ts = 3$. Similarly, the third and forth time slots are allocated to n_2 and n_1, respectively, as shown in **Fig. 12b**.

Fig. 12 however does not cover the case of step (3) in **Fig. 10**. In order to explain this step, another example shown in **Fig. 13** will be used. After the GTS allocation for *L_nodes* (n_4~n_{11}), the algorithm in **Fig. 10** starts. In step (1), *DA_S* becomes $\{n_1, n_2, n_3\}$ and the third time slot is allocated to n_1 in step (2). In step (3), n_3 is selected as n_{LCN} and n_2 as n_{HCN}, so that n_3 can transmit its data to n_2 while n_1 delivers data to the sink node. Next, based on steps (1) and (2) in **Fig. 10**, n_2 delivers aggregated data to the sink node at $ts = 4$.

4. Performance Evaluation

Our performance evaluation is based on both mathematical analysis and implementation. For the mathematical analysis, ISRMC-MAC is compared with HyMAC [19] and the base MAC protocol, which is the TDMA-based single channel MAC protocol. Section 2 discussed several single-radio multi-channel MAC protocols, and among them HyMAC showed the best performance. For the implementation, the performance of ISRMC-MAC is compared with the IEEE 802.15.4 MAC protocol. The parameters for the performance evaluation are as follows: The number of available channels is 1 ~ 16 and the number of sensor nodes is 1 ~ 64. The Beacon Order and Superframe Order of the superframe structure is set to 10, and thus, the duration of a time slot is 62 ms. In addition, each sensor node is assumed to concurrently transmit data during each superframe after the beacon transmission completes. Finally, the data size is assumed to be 5 bytes.

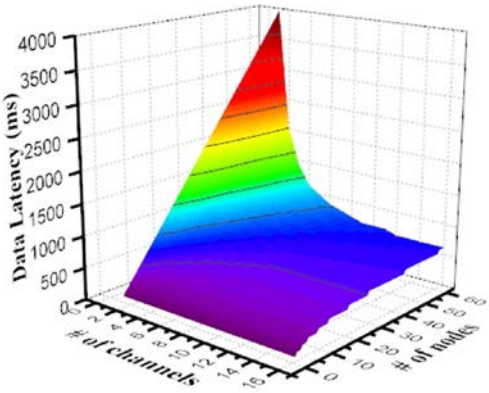

(b) HyMAC.

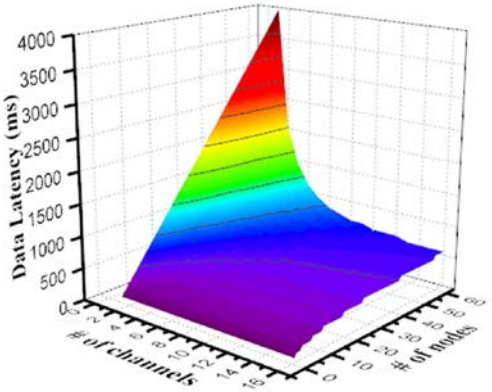

(c) ISRMC.

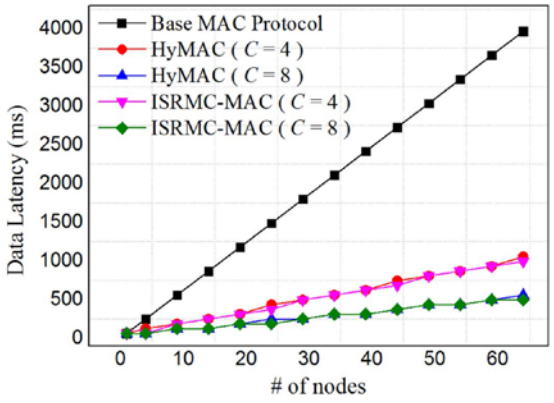

(a) Comparison.

Fig. 14. Analytical result on data latency.

4.1 Analytical Analysis

This subsection verifies through mathematical analysis that ISRMC-MAC reduces latency compared with the base MAC protocol and increases energy efficiency compared with HyMAC.

4.1.1 Data Latency

All of the compared MAC protocols use the TDMA-based approach, and thus, the latency as function of N and C ($T_{(N,C)}$) is defined by

$$T_{(N,C)} = G_{(N,C)} \times Duration\ of\ a\ GTS\ (\text{in}\ ms), \tag{1}$$

where $G_{(N,C)}$ represents the maximum number of time slots required for N sensor nodes given C channels.

$G_{(N,1)}^{Base}$ for the base MAC protocol is defined by the following equation:

$$G_{(N,1)}^{Base} = N. \tag{2}$$

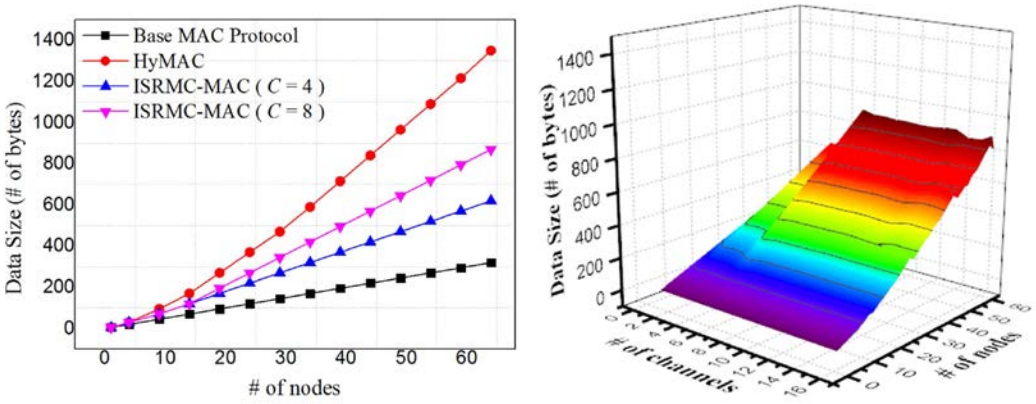

(a) Comparison. (b) ISRMC.

Fig. 15. Analytical result on data size.

The base MAC protocol uses the star topology with a single-channel, and thus, the number of time slots required is the same as the number of sensor nodes (N).

In contrast, ISRMC-MAC and HyMAC reduce data latency compared to the base MAC protocol by concurrently transmitting data using multi-channel communication. Therefore, $\left\lceil \frac{N}{C} \right\rceil$ time slots are required in each channel when parallel transmissions are fully exploited.

Since deriving exact equations for $G_{(N,C)}^{HyMAC}$ and $G_{(N,C)}^{ISRMC}$ is impractical, they are manually calculated for $1 \leq N \leq 64$ and $1 \leq C \leq 64$. These results shown in **Fig. 14** indicate that (1) both ISRMC-MAC and HyMAC have similar performance on data latency, and (2) multi-channel protocols are superior to single-channel protocols in terms of data latency.

4.1.2 Energy Efficiency

Most of the energy consumption occurs during communication. Since the multi-channel approach relies on data duplication to reduce data latency, the number of packets and the total data size affect energy consumption. The analytical analysis in Subsection 4.1.1 reveals that the number of packets for HyMAC and ISRMC-MAC are similar because the required number of time slots for the two methods are almost the same. However, this subsection shows that the proposed ISRMC-MAC outperforms HyMAC in terms of energy efficiency because the total data size is decreased.

Assuming that the packet size is constant, the total data size, $D_{(N,C)}$, is defined as the total number of data duplications required for all the transmissions of N sensor nodes using C channels including original packets from the sensor nodes. In fact, $D_{(N,C)}$ is equivalent to N original packets plus the total number of hops for all the transmissions. The total data size $DS_{(N,C)}$ can be expressed as follows:

$$DS_{(N,C)} = D_{(N,C)} \times Packet\ size\ (\text{in}\ bytes). \tag{3}$$

Since there is no data duplication in the base MAC protocol, $DS_{(N,1)}^{Base}$ simply increases linearly as function of N.

HyMAC employs the binary tree topology; therefore, its total data size $D_{(N,C)}^{HyMAC}$ is given by the following equations:

$$D_{(1,C)}^{HyMAC} = 1$$
$$D_{(N,C)}^{HyMAC} = D_{(N-1,C)}^{HyMAC} + 1 + \lfloor \log_2(N+1) \rfloor, \text{for } N \geq 2 \quad (4)$$

where $\lfloor \log_2(N+1) \rfloor$ indicates the level of the binary tree.

Finally, the total data size for the proposed ISRMC-MAC, $D_{(N,C)}^{ISRMC}$, can be expressed as follows:

$$D_{(N,C)}^{ISRMC} = \lceil \log_2 N \rceil, \text{for } 1 \leq N \leq C$$
$$D_{(N,C)}^{ISRMC} = D_{(N-1,C)}^{ISRMC} + 1 + \lceil \log_2(C-1) \rceil, \text{for } N \geq C \quad (5)$$

In the proposed *Unbalanced Star+Mesh topology*, there are no *L_nodes* when $N < C$, i.e., only the sink node and *DA_nodes* exist. In this case, N *DA_nodes* aggregate data among each other resulting in maximum of $\lceil \log_2 N \rceil$ data duplications.

When $N \geq C$, *L_nodes* exist and one data duplication for each *L_node* occurs at *DA_nodes*,

Fig. 16. Sensor node platform: ZigbeX.

and additional data duplications occur among *DA_nodes* in the mesh topology. Since the number of *DA_nodes* is $C - 1$, the upper bound on the number of additional duplications is $\lceil \log_2(C-1) \rceil$.

Comparison of Eqs. 4 and 5 shows that the proposed ISRMC-MAC protocol is superior to HyMAC in terms of energy consumption because $D_{(N,C)}^{HyMAC}$ depends on N but $D_{(N,C)}^{ISRMC}$ depends on C. **Fig. 15** shows the calculated values of $D_{(N,C)}^{HyMAC}$ and $D_{(N,C)}^{ISRMC}$ for $1 \leq N \leq 64$ and $1 \leq C \leq 64$, which reveals that the above analysis holds.

4.2 Implementation

The proposed ISRMC-MAC protocol has been implemented and tested on ZigbeX shown in **Fig. 16**. ZigbeX consists of an ATMega128L microcontroller and a CC2420 transceiver, which supports a single-radio with multiple channels. The number of channels (C) supported is 4 and the number of nodes (N) varies from 1 to 15. The nodes are randomly deployed in 1m × 0.5m space representing a human body. All the nodes utilize the same power level 7, which is the lowest power available on the CC2420 module. Our experiments consider data latency and energy efficiency to verify the performance of the proposed method.

4.2.1 Data Latency

Fig. 17a shows the data latency versus N when C is fixed to 4. The latency for the base MAC protocol significantly increases as the number of sensor nodes increases. For example, when N = 15, the latency is 1,032 ms. On the other hand, the latency for ISRMC-MAC increases

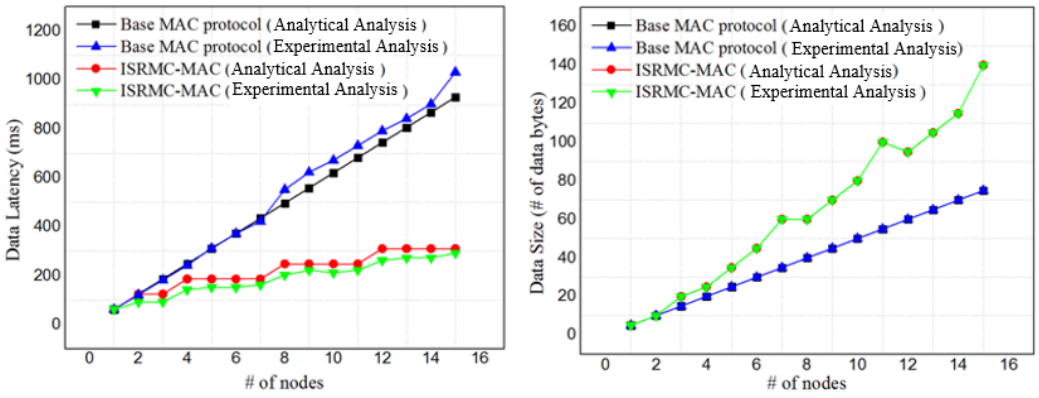

(a) Data latency. (b) Data Size.

Fig. 17. Experimental results.

slowly due to the multi-channel approach. The gap between the two methods also increases as N increases. When N = 15, the latency of ISRMC-MAC is 292 ms. These results verify that the proposed ISRMC-MAC protocol significantly reduces data latency compared with existing single-channel approaches.

Note that the analytical results of ISRMC-MAC derived in Subsection 4.1.1 are the upper bounds on data latency, thus they are higher than the experimental results as shown in **Fig. 17(a)**.

4.2.2 Energy Efficiency

Fig. 17b shows the total data size versus N when C is fixed to 4. As can be seen, ISRMC-MAC transmits more data than the base MAC protocol. Again, this is because the base MAC protocol uses a TDMA-based single-channel star topology, and thus, there is no data duplication. On the other hand, the Unbalanced Star+Mesh topology of ISRMC-MAC requires data aggregation, which increases the total data size. However, the results from our implementation are very similar to the mathematical analysis, which verifies that our proposed method improves energy efficiency compared to other single-radio multi-channel MAC protocols.

5. Conclusion

WBAN is a promising wireless technology to satisfy the requirements of healthcare applications. However, high density of sensor nodes in a WBAN can cause energy inefficiency and high data latency. Many MAC protocols have been proposed to alleviate these problems, but none of these methods fully satisfy all the requirements of WBANs. Some of them employ multi-radio technique, but they are not feasible using off-the-shelf radios. Others employ single-radio and data aggregation, but energy consumption increases due to data duplication. The proposed ISRMC-MAC protocol uses a single-radio, multichannel approach, which can be implemented on off-the-shelf sensor devices. Moreover, the Unbalanced Star+Mesh topology together with channel and GTS allocation strategies reduces data duplication by reducing the number hops. Therefore, the proposed approach improves throughput using the multi-channel and reduces energy consumption by decreasing data duplication.

The superiority of ISRMC-MAC over the state-of-the-art protocol HyMAC was validated through mathematical analyses and experiments using ZigbeX. Our results showed that the proposed method reduces data latency and improves energy efficiency compared to HyMAC by achieving more than two-fold reduction in data duplication.

References

[1] IEEE Computer Society, *IEEE Standard for Local and metropolitan area networks - Part 15.6: Wireless Body Area Networks (WBANs)*, LAN/MAN Standards Committee, New York, 2012.

[2] W. B. Heinzelman, A. P. Chandrakasan, and H. Balakrishnan, "An Application-Specific Protocol Architecture for Wireless Microsensor Network," *IEEE Transactions on Wireless Communications*, vol.1, no.4, pp. 660-670, October 2002. Article (CrossRef Link)

[3] G. Fang and E. Dutkiewicz, "BodyMAC: Energy Efficient TDMA-based MAC Protocol for Wireless Body Area Networks," *International Symposium on Communications and Information Technology*, pp. 1455-1459, September 28-30, 2009. Article (CrossRef Link)

[4] S. Marinkovic, C. Spagnol, and E. Popovici, "Energy-Efficient TDMA-based MAC Protocol for Wireless Body Area Networks," in *Proc. of International Conference on Sensor Technologies and Applications*, pp. 604-609, June 18-23, 2009. Article (CrossRef Link)

[5] Y. Tselishchev L. Libman, and A. Boulis, "Energy-Efficient Retransmission Strategies under Variable TDMA Scheduling in Body Area Networks," in *Proc. of IEEE Conference on Local Computer Networks*, pp. 374-381, October 4-7, 2011. Article (CrossRef Link)

[6] W. Ye, J. Heidemann, and D. Estrin, "An Energy-Efficient MAC Protocol for Wireless Sensor Networks," in *Proc. of IEEE International Conference on Computer Communications*, pp. 1567-1576, June 23-27, 2002. Article (CrossRef Link)

[7] J. Polastre, J. Hill. and D. Culler, "Versatile Low Power Media Access for Wireless Sensor Networks," in *Proc. of IEEE International Conference on Embedded networked sensor systems*, pp. 95-107, November 3-5, 2004. Article (CrossRef Link)

[8] D. L. Wei, Y. C. Jin, S. Vural, K. M. Moessner, and R. Tafazolli, "An energy-efficient clustering solution for wireless sensor networks," *IEEE Tran. Wireless Communications*, vol. 10, no. 11, pp. 3973-3983, November 2011. Article (CrossRef Link)

[9] A. El-Hoiydi and J.-D Decotignie, "WiseMAC: An Ultra Low Power MAC Protocol for the Downlink of Infrastructure Wireless Sensor Networks," in *Proc. of International Symposium on Computers and Communications*, pp. 244-251, June 28 – July 1, 2004. Article (CrossRef Link)

[10] S. M. Yoo, C. J. Chen, and P. H. Chou, "Low-Complexity, High-Throughput Multiple-Access Wireless Protocol for Body Sensor Networks," in *Proc. of International Workshop on Wearable and Implantable Body Sensor Networks*, pp. 109-113, June 3-5, 2009. Article (CrossRef Link)

[11] C. Li, H. B. Li, and R. Kohno, "Reservation-Based Dynamic TDMA Protocol for Medical Body Area Networks," *IEICE Transactions on Communications*, Vol.E92-B, No.2, pp. 387-395, February 2009. Article (CrossRef Link)

[12] Y. Tselishchev, L. Libman, and A. Boulis, "Reducing Transmission Losses in Body Area Networks using Variable TDMA Scheduling," in *Proc. of IEEE International Symposium on World of Wireless, Mobile and Multimedia Networks*, pp. 1-10, June 20-24, 2011. Article (CrossRef Link)

[13] P. Suriyachai, U. Roedig, and A. Scott, "A Survey of MAC Protocols for Mission-Critical Applications in Wireless Sensor Networks," *IEEE Communications Survey & Tutorials*, vol. 14, no. 2, pp. 240-264, March 2011. Article (CrossRef Link)

[14] M. Chen, S. Gonzalez, A. Vasilakos, C. Huasong, and C. Victor, and M. Leung, "Body Area Networks: A Survey," *Mobile Networks and Applications*, vol. 16, no. 2, pp. 171-193, August 2010. Article (CrossRef Link)

[15] S. Ullah *et al.*, "A Comprehensive Survey of Wireless Body Area Networks," *Journal of Medical Systems*, vol. 36, no. 3, pp. 1065-1094, August 2010. Article (CrossRef Link)

[16] Y. Kim, H. Shin and H. Cha, "Y-MAC: An Energy-efficient Multi-channel MAC Protocol for Dense Wireless Sensor Networks," in *Proc. of International Conference on Information Processing in Sensor Networks*, pp. 53-63, April 22-24, 2008. Article (CrossRef Link)
[17] O. Durmaz Incel, L. van Hoesel, P. Jansen and P. Havinga, "MC-LMAC: A Multi-Channel MAC Protocol for Wireless Sensor Networks," *Journal of Ad Hoc Networks*, vol. 9, no. 1, pp. 73-94, January 2011. Article (CrossRef Link)
[18] L. F. W. van Hoesel and P. J. M. Havinga, "A Lightweight Medium Access Protocol (LMAC) for Wireless Sensor Networks: Reducing Preamble Transmissions and Transceiver State Switches," in *Proc. of International Workshop on Networked Sensing Systems*, pp. 205-208, June 22-23, 2004. Article (CrossRef Link)
[19] G. Zhou, C. Huang, T. Yan, T. He, and J. A. Stankovic, "MMSN: Multi-Frequency Media Access Control for Wireless Sensor Networks," in *Proc. of IEEE International Conference on Computer Communications*, pp. 1-13, April 23-29, 2006. Article (CrossRef Link)
[20] M. Salajegheh, H. Soroush, and A. Kalis, "HyMAC: Hybrid TDMA/FDMA Medium Access Control Protocol for Wireless Sensor Networks," in *Proc. of International Symposium on Indoor and Mobile Radio Communications*, pp. 1-5, September 3-7, 2007. Article (CrossRef Link)
[21] J. Borms, K. Steenhaut and B. Lemmens, "Low-Overhead Dynamic Multi-channel MAC for Wireless Sensor Networks," in *Proc. of European Conference on Wireless Sensor Networks*, pp. 81-96, February 17-19, 2010. Article (CrossRef Link)
[22] Y. Wu, J. A. Stankovic, T. He, and S. Lin, "Realistic and Efficient Multi-Channel Communications in Wireless Sensor Networks," in *Proc. of IEEE International Conference on Computer Communications*, pp. 1867-1875, April 13-18, 2008. Article (CrossRef Link)
[23] L. Cheng and P. Wang, "A Cluster Based On-demand Multi-Channel MAC Protocol for Wireless Multimedia Sensor Networks," in *Proc. of IEEE International Conference on Communications*, pp. 2371-2376, May 19-23, 2008. Article (CorssRef Link)
[24] W. Lee, S. H. Rhee, Y. Kim, and H. Lee, "An Efficient Multi-channel Management Protocol for Wireless Body Area Networks," in *Proc. of International Conference on Information Networking*, pp. 13-17, January 20-23, 2009. Article (CrossRef Link)
[25] I. Kirbas, A. Karahan, A. Sevin, and C. Bayilmis, "isMAC: An Adaptive and Energy-Efficient MAC Protocol Based on Multi-Channel Communication for Wireless Body Area Networks," *KSII Transactions on Internet and Information Systems*, vol. 7, no. 8, pp. 1805-1824, August 2013. Article (CrossRef Link)
[26] IEEE Computer Society, *Part 15.4: Low-Rate Wireless Personal Area Networks (LR-WPANs)*, LAN/MAN Standards Committee, New York, 2011.

Kunryun Cho received the B.S. and M.S. degree in computer engineering from Kyung Hee University, Korea, in 2012 and 2014. He is currently pursuing the Ph.D. degree with the Department of Computer Engineering, Seoul National University, Korea. His research interests include wireless sensor network, wireless body area network, wireless local area network, and indoor localization.

Seokhee Jeon received the BS and PhD degrees in computer science and engineering at the Pohang University of Science and Technology (POSTECH) in 2003 and 2010, respectively. From 2010 to 2012, he was a postdoctoral researcher in the Computer Vision Laboratory at ETH Zurich. In 2012, he joined as an assistant professor in the Department of Computer Engineering, Kyung Hee University, where he is currently directing the Haptics Laboratory. His research focuses on haptic rendering in an augmented reality environment, applications of haptics technology in medical training, and usability of augmented reality applications.

Jinsung Cho (M'15) received the B.S., M.S, and Ph.D. degrees in computer engineering from Seoul National University, Korea, in 1992, 1994, and 2000, respectively. He was a Visiting Researcher with the IBM T. J. Watson Research Center, in 1998, and a member of the Research Staff with Samsung Electronics, from 1999 to 2003. He is currently a Professor with the Department of Computer Engineering, Kyung Hee University, Korea. His research interests include mobile networking and computing, embedded systems and software, and sensor and body networks.

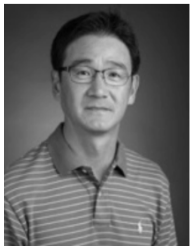

Ben Lee received the B.E. degree in electrical engineering from the Department of Electrical Engineering, State University of New York (SUNY) at Stony Brook, in 1984, and the Ph.D. degree in computer engineering from the Department of Electrical and Computer Engineering, Pennsylvania State University, in 1991. He is currently a Professor of School of Electrical Engineering and Computer Science with Oregon State University. His research interests include wireless networks, embedded systems, computer architecture, multimedia systems, and parallel and distributed systems. He received the Loyd Carter Award for Outstanding and Inspirational Teaching and the Alumni Professor Award for Outstanding Contribution to the College and the University from the OSU College of Engineering, in 1994 and 2005, respectively. He also received the HKN Innovative Teaching Award from Eta Kappa Nu, School of Electrical Engineering and Computer Science, in 2008. He has been on the Program and Organizing Committees for numerous international conferences, including the 2003 International Conference on Parallel and Distributed Computing Systems, the 2005–2011 IEEE Workshop on Pervasive Wireless Networking, and the 2006, 2007, and 2009 IEEE International Conference on Pervasive Computing and Communications. He was also a Keynote Speaker at the 2014 International Conference on Ubiquitous Information Management and Communication. He is currently the Chair of the Social, P2P and Multimedia Networking, Services and Applications track for the 2016 IEEE Consumer Communications and Networking Conference.